2790-1688

ISEEMS 2023

Volume-8-(2023)

Three-dimensional Electrocatalytic Degradation of Tetracycline by Nano-Feooh

Qiang Xu[1,*], Yuexin Wang[1], Yanming Zhou[1], Yucai Gong[1], Dewen Kong[1], Shoufeng Tang[2], Qingrui Zhang[2]

[1] Tangshan Jiahua coal chemical Co., LTD, Tangshan, 063611, PR China;

[2] Hebei Key Laboratory of Heavy Metal Deep-remediation in Water and Resource Reuse, School of Environmental and Chemical Engineering, Yanshan University, Qinhuangdao, 066004, PR China.

[*] yyy981014@163.com

Abstract. Nano-FeOOH catalysts were prepared by a co-precipitation method and characterized by XRD, SEM, XPS and BET to analyze the phase composition, surface morphology, elemental composition and specific surface area of FeOOH. Results showed that the FeOOH catalyst had large pore volume and surface area, providing more active sites for catalytic reactions. A 3D electrocatalytic system EC/PS/FeOOH was established to degrade tetracycline (TC), and the contributions of FeOOH adsorption, PS activation and electrocatalysis were investigated. It was found that the adsorption rate of TC on sole FeOOH was 42%, the degradation rate of TC in the PS/FeOOH system was 63.80%, and the degradation rate of TC in the 3D EC/PS/FeOOH system reached 72.97%, indicating the high electrocatalytic activity of FeOOH. Surface catalysis mechanism studies showed that the high catalytic activity of FeOOH could be attributed to electron transfer between Fe(II) and Fe(III) and adsorbed oxygen on its surface.

Keywords: nano-FeOOH; tetracycline; electrocatalytic oxidation; heterogeneous Fenton; persulphate.

1. Introduction

Tetracycline (TC) is one of the most widely used antibiotics in human applications. Current research shows that TC can be detected in groundwater, surface water, soil and sediments [1]. The overuse of TC can easily lead to the emergence of antibiotic-resistant bacteria, posing huge threats to the ecological environment.

Electrocatalytic oxidation technology (EC) features high treatment efficiency, no secondary pollution, good environmental compatibility and applicability, and has become a very promising organic wastewater treatment technology. Traditional homogeneous electrocatalytic systems have some disadvantages such as narrow applicable pH range, the need for adding large amounts of electrolytes, easy formation of iron mud by Fe2+ causing secondary pollution, etc [2].

EC can not only directly oxidize organics, but also activate persulfate (PS) to generate SO4•- through electron transfer to degrade organics [3]. This multifunctional synergetic mechanism of EC coupling PS can achieve better degradation of organics. In addition, heterogeneous electrocatalytic activation is also a very promising way other than the conventional electroactivation of PS. Introduction of heterogeneous electrocatalysts into the EC system to form three-dimensional electrocatalytic systems can not only improve the utilization of catalysts and oxidants, but also significantly enhance the degradation efficiency of organics. Moreover, FeOOH has been extensively studied due to its high reactivity, low cost and easy preparation [4], and has proven to be an excellent iron-based catalyst.

In view of the limitations of traditional EC, this study prepared FeOOH iron-based catalysts and characterized them, established a three-dimensional electrocatalytic EC/PS/FeOOH system, chose TC as the target pollutant, and investigated the performance and mechanism of the synergistic system in degrading TC.

2. Materials and Methods

Nano-FeOOH catalysts were prepared by a coprecipitation method [5]. 5.5604 g of $FeSO_4·7H_2O$ was dissolved in 100 mL of deionized water, and 3 mol L^{-1} NaOH solution was added dropwise under magnetic stirring until the pH of the solution was maintained at around 11. The reaction temperature was controlled at 30-40°C. After complete precipitation, the solution was aged for 1-3 h, then washed, filtered and dried at constant temperature for 12 h to obtain the nano-FeOOH catalysts.

The crystalline structure of the catalysts was determined by X-ray diffraction (XRD) using a D-max-2500/PC diffractometer (Rigaku, Japan). The obtained patterns were matched with standard patterns in the database for phase identification. A SUPRA55 SAPPHIRE scanning electron microscope (SEM) (Carl Zeiss, Germany) was used to characterize the surface morphology and particle dispersion of the iron-based catalysts. The specific surface area (SSA, m^2 g^{-1}) of the catalysts was measured by an ASAP2020 surface area analyzer (BET, Micromeritics, USA). The BET (Brunauer-Emmett-Teller) method was used to calculate the specific surface area and pore size distribution of the catalysts. An AXIS Ultra DLD X-ray photoelectron spectrometer (XPS, Kratos, UK) was used to determine the elemental composition and valence states of the catalysts.

The prepared FeOOH catalysts were introduced into the homogeneous EC/PS electrocatalytic system to construct a heterogeneous electrocatalytic system using TC as the target pollutant for degradation experiments. In the reactor, 100 mL TC simulated wastewater of a certain concentration was prepared and the pH was adjusted. A certain amount of iron-based catalyst was added to the reactor and dispersed uniformly in the solution by magnetic stirring. The applied voltage, amounts of PS, catalyst dosage, and initial pH were controlled. The DC power supply was turned on and samples were taken every 10 min during the experiment to measure TC concentration and calculate the degradation rate.

The PS concentration was determined by iodometric method as follows: 2 mL sample solution was taken into a 50 mL colorimetric tube, 0.2 g $NaHCO_3$ and 4 g KI were immediately added, then deionized water was added to the 50 mL mark. The tube was shaken to mix uniformly and allowed to stand for color development for 15 min in the dark. The absorbance was measured at 352 nm.

The absorbance of TC was measured by UV-vis spectrophotometry at 356 nm. The degradation rate of organics was calculated using the following formula:

$$\eta = \frac{C_0 - C_t}{C_0} \times 100\% \qquad （1）$$

where, η is degradation rate (%), C_0 represents initial concentration of organics (mg L^{-1}), C_t is concentration of residual organics after reaction for t min (mg L^{-1}).

3. Results and Discussion

The crystalline structure of the synthesized FeOOH was analyzed by XRD patterns. As shown in Figure 1, FeOOH exhibited distinct diffraction peaks at 21.2°, 33.2°, 36.0°, 41.2°, 53.2° and 59.0°, which is consistent with the standard PDF card (JCPS No.29-0713). This indicates that the FeOOH catalysts synthesized by coprecipitation have high purity and good crystalline morphology. The morphological characteristics and structure of FeOOH were observed by scanning electron microscopy (Figure 2). The prepared FeOOH showed quasi-spherical shape, and the size distribution was not uniform due to aggregation of individual particles.

The porous structure of FeOOH was investigated by N2 adsorption-desorption experiments. As shown in Figure 3, according to IUPAC classification, the curve was identified as type IV adsorption isotherm with H3-type hysteresis loops, indicating that FeOOH has a mesoporous structure. Table 1 summarizes the specific surface area, pore volume and average pore diameter of FeOOH. It can be seen that FeOOH has a large pore volume and developed specific surface area. The high specific surface area can provide more active sites, thereby promoting mass transfer of reactants on the catalyst surface and ensuring high catalytic performance of the catalyst [6].
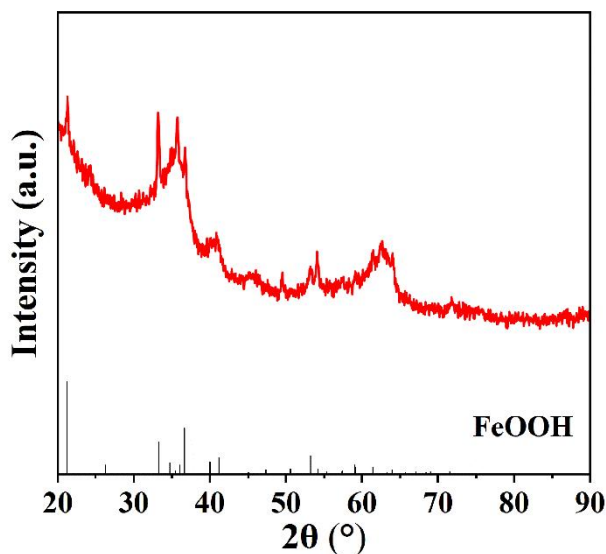
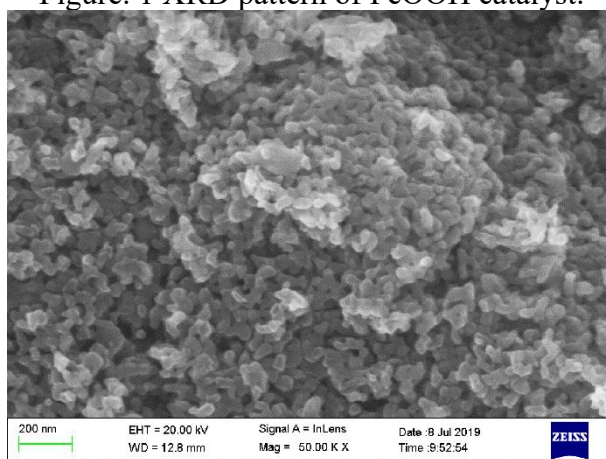Figure. 1 XRD pattern of FeOOH catalyst.
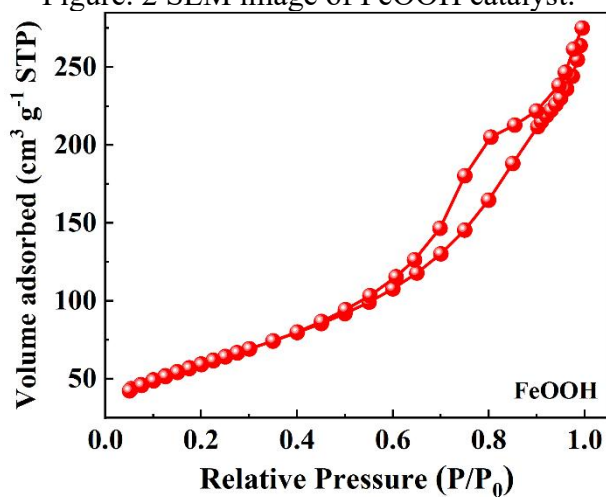

Figure. 2 SEM image of FeOOH catalyst.

Figure. 3 N$_2$ adsorption-desorption curves of FeOOH.

Table 1. The pore analysis and specific surface area of FeOOH.

Catalyst	Surface area （m^2 g^{-1}）	Pore volume （cm^3 g^{-1}）	Average pore diameter （nm）
FeOOH	218.08	0.42	27.51

Figure 4 shows the effect of solution pH on the adsorption capacity of FeOOH, where the initial pH of 25 mg/L TC was 4.5. The results showed that the adsorption performance of the catalyst was highly dependent on the solution pH. Under the initial pH condition of TC, FeOOH exhibited good adsorption performance with adsorption capacities of 52.46 mg/g. When the pH increased from 4.5 to 7.0, the adsorption capacity of FeOOH remained almost unchanged at about 51.24 mg/g. However, as the pH further increased to 9.0, the adsorption capacity of FeOOH decreased significantly to 26.85 mg/g. FeOOH had the highest adsorption capacity under acidic conditions, while alkaline conditions significantly inhibited the adsorption of TC on the catalyst. This difference in adsorption performance caused by different pH is due to the amphoteric nature of TC. The existence form of TC in solution depends on the pH, being protonated form (TC+) under acidic conditions and single anionic form (TC-) under alkaline conditions. Therefore, when the pH was 9.0, the electrostatic repulsion would lead to a significant decrease in the adsorption capacity of the catalyst [7].
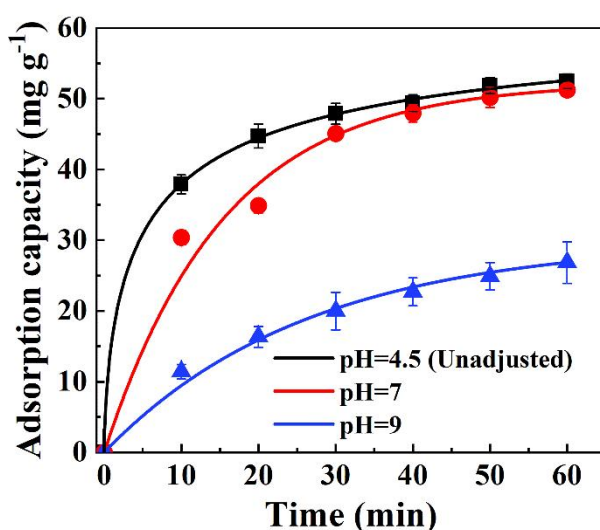

Figure. 4 Adsorption isotherm curve of FeOOH at different pH values.

FeOOH was used as an activator of PS to investigate its degradation effect on TC. As shown in Figure 5, the degradation rate of TC was 63.80% in the PS/FeOOH system. The higher TC removal rate in the PS/FeOOH system could be attributed to the high adsorption capacity of FeOOH. In addition, the decomposition amount of PS was measured. The decomposition amount of PS was 0.11 mmol L−1 in the PS/FeOOH system, indicating that FeOOH can effectively activate PS.
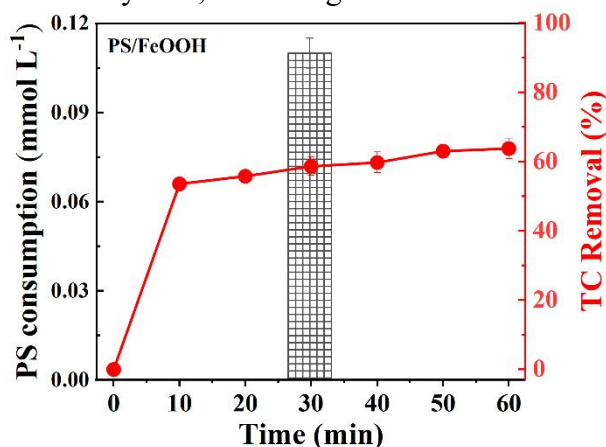

Figure. 5 The degration efficiency of TC and decomposition capacity of PS in PS/FeOOH.

Figure 6 evaluates the electrocatalytic performance of FeOOH, i.e. investigating its degradation effect on TC under the heterogeneous electrocatalytic activation PS system. The degradation rate of TC reached 72.97% in the EC/PS/FeOOH system. Notably, despite the large TC adsorption

capacity, FeOOH did not achieve a good synergistic degradation effect, indicating that the degradation of TC in the heterogeneous electrocatalytic system relied mainly on oxidative degradation rather than adsorptive degradation. To assess the impacts of adsorption and oxidation on TC degradation, the above data were reintegrated to estimate the characteristics and relative contributions of different active components in the system, as shown in Figure 6. By coupling adsorption and PS activation, the EC/PS/FeOOH system can promote the degradation of TC.
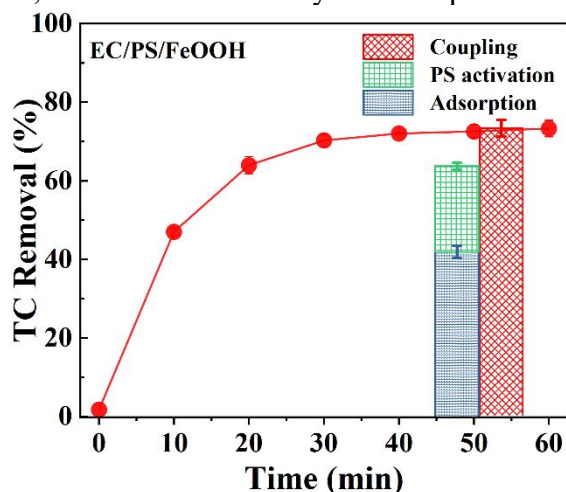

Figure. 6 TC degradation rate and contribution rate in ES/PS/FeOOH collaborative system.

In order to further understand the elemental chemical states and electronic characteristics of the catalyst surface, XPS tests were performed on the catalyst before and after use. Figure 7(a) shows the full XPS spectrum of FeOOH, indicating that the prepared FeOOH contains three elements of Fe, O and C, where the C 1s peak may be due to contamination during sample preparation.

Figure 7(b) shows the XPS spectra of Fe in FeOOH before and after the reaction. It can be seen that before the reaction, the two characteristic peaks of Fe 2p3/2 and Fe 2p1/2 in FeOOH located at 711.8 eV and 724.7 eV correspond to Fe(III) [8], indicating that FeOOH mainly existed in the form of Fe(III). After the reaction, the change in Fe valence states in FeOOH can be clearly observed, suggesting that Fe(III) in FeOOH had been converted to mixed Fe(II) and Fe(III) states, with 31.17% of Fe(II). This means that Fe(III) is the main catalytic active center, and the mutual conversion between Fe(II) and Fe(III) can better achieve electron transfer to activate PS (Eq. 2-3) [9]. In Figure 7(c), the O 1s peak of FeOOH shows two spectral bands at 529.5 eV and 531.5 eV, attributed to lattice oxygen and adsorbed oxygen, respectively [10]. Compared with lattice oxygen, adsorbed oxygen has higher mobility and can actively participate in multiphase catalysis processes. In the spectrum of FeOOH after the reaction, the content of adsorbed oxygen increased from 45.97% to 55.03%, and the increase in adsorbed oxygen content may lead to enhanced catalytic activity.
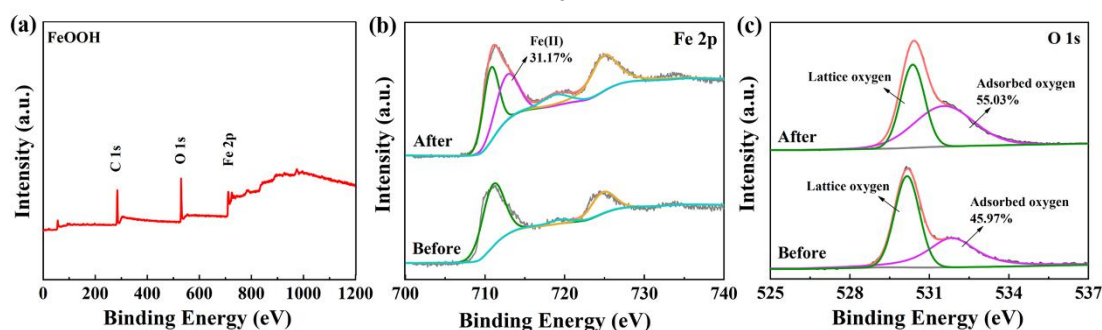
$$\equiv Fe(III) + e^- \rightarrow \equiv Fe(II) \qquad\qquad (2)$$

$$\equiv Fe(II) + S_2O_8^{2-} \rightarrow \equiv Fe(III) + SO_4^{\bullet-} + SO_4^{2-} \qquad\qquad (3)$$

Figure. 7 (a) XPS survey spectrum of FeOOH, (b) XPS Fe 2p spectra, and (c) XPS O 1s spectra.

4. Conclusion

This study prepared FeOOH catalysts by coprecipitation and constructed an EC/PS/FeOOH system to degrade TC. The phase composition, surface morphology, elemental composition and specific surface area of FeOOH were investigated by characterization techniques including XRD, SEM, XPS, and BET. The results demonstrated the successful preparation of FeOOH catalysts. The adsorption, activation and electrocatalytic performances of FeOOH catalysts were examined. It was found that FeOOH exhibited good adsorption performance and high electrocatalytic activity. The surface catalysis mechanism analysis showed that the high catalytic activity of FeOOH could be attributed to electron transfer between Fe(II) and Fe(III) and increased adsorbed oxygen, thus promoting the degradation of TC.

References

[1] N. Mosaleheh, M.N. Sarvi, Minimizing the residual antimicrobial activity of tetracycline after adsorption into the montmorillonite: Effect of organic modification, ENVIRON RES, 182 (2020) 109056.

[2] C. Kim, J. Ahn, T.Y. Kim, I. Hwang, Mechanisms of electro-assisted persulfate/nano-Fe0 oxidation process: Roles of redox mediation by dissolved Fe, J HAZARD MATER, 388 (2020) 121739.

[3] Y. Chen, Y. Li, Y. Wang, I.Y. Zhang, R. Huang, Efficient removal of recalcitrant naphthenic acids with electro-cocatalytic activation of peroxymonosulfate by Fe(III)-nitrilotriacetic acid complex under neutral initial pH condition, J HAZARD MATER, 455 (2023) 131524.

[4] C. Li, J. Wu, W. Peng, Z. Fang, J. Liu, Peroxymonosulfate activation for efficient sulfamethoxazole degradation by Fe_3O_4/β-FeOOH nanocomposites: Coexistence of radical and non-radical reactions, CHEM ENG J, 356 (2019) 904-914.

[5] H. Zhang, J. Wang, X. Zhang, B. Li, X. Cheng, Enhanced removal of lomefloxacin based on peroxymonosulfate activation by Co_3O_4/δ-FeOOH composite, CHEM ENG J, 369 (2019) 834-844.

[6] R. Li, W. Li, C. Jin, Q. He, Y. Wang, Fabrication of ZIF-8@TiO2 micron composite via hydrothermal method with enhanced absorption and photocatalytic activities in tetracycline degradation, J ALLOY COMPD, 825 (2020) 154008.

[7] Y. Guo, C. Yan, P. Wang, L. Rao, C. Wang, Doping of carbon into boron nitride to get the increased adsorption ability for tetracycline from water by changing the pH of solution, CHEM ENG J, 387 (2020) 124136.

[8] J. Hu, J. Li, J. Cui, W. An, L. Liu, Y. Liang, W. Cui, Surface oxygen vacancies enriched FeOOH/Bi2MoO6 photocatalysis- fenton synergy degradation of organic pollutants, J HAZARD MATER, 384 (2020) 121399.

[9] H. Lin, H. Zhang, L. Hou, Degradation of C. I. Acid Orange 7 in aqueous solution by a novel electro/Fe3O4/PDS process, J HAZARD MATER, 276 (2014) 182-191.

[10] H. Fu, P. Zhao, S. Xu, G. Cheng, Z. Li, Y. Li, K. Li, S. Ma, Fabrication of Fe3O4 and graphitized porous biochar composites for activating peroxymonosulfate to degrade p-hydroxybenzoic acid: Insights on the mechanism, CHEM ENG J, 375 (2019) 121980.